

# Local trade-off between information and disturbance in quantum measurements

Hiroaki Terashima

*Department of Physics, Cooperative Faculty of Education,  
Gunma University,  
Maebashi, Gunma 371-8510, Japan*

## Abstract

This study confirms a local trade-off between information and disturbance in quantum measurements, and establishes the correlation between the changes in these two quantities when the measurement is slightly modified. The correlation indicates that when the measurement is modified to increase the obtained information, the disturbance also increases. However, the information can be increased while decreasing the disturbance because the correlation is not necessarily perfect. For measurements with imperfect correlation between the information and disturbance, this paper discusses a general scheme that raises the amount of information in the measurement while diminishing the disturbance.

## 1 Introduction

An interesting topic in the quantum theory of measurements is the trade-off between information and disturbance. In general, when a measurement outcome provides much information about the state of a system, it causes a large disturbance in the state of the system. This trade-off has been studied using various measures of information and disturbance [1–18]. For example, the information can be quantified by estimation fidelity, which defines the similarity between the actual state and an estimated state based on the outcome. Similarly, the disturbance can be quantified by operation fidelity, defining the similarity between the original state and the disturbed state after a measurement, or by physical reversibility, defining the recovery probability of the original state after a reverse operation on the disturbed state. These quantities are known to satisfy inequalities [2, 15] that represent the trade-off.

Most studies on the information–disturbance trade-off are focused on optimal measurements, which saturate the upper bound of the information for

a given disturbance. The optimal measurements correspond to the upper boundary of the region obtained by plotting all physically possible measurements on an information–disturbance plane [19]. An optimal measurement providing more information always causes a larger disturbance in the system, as seen from the slope of the upper boundary of the region [20]. However, this rule is violated for the non-optimal measurements in the interior of the region. Within the neighborhood of a non-optimal measurement, there always exists another measurement that provides more information with smaller disturbance. Although the information and disturbance of non-optimal measurements are correlated to some extent, the relationship is imperfect.

This paper presents a local trade-off between information and disturbance in quantum measurements by correlating their changes when the measurement is slightly modified. When the measurement is performed on a quantum system in a completely unknown state, the obtained information and resulting disturbance are represented as functions of the singular values of a measurement operator corresponding to the outcome. Using the gradient vectors of these functions, we plot the information changes versus disturbance changes on a plane for various modifications of the measurement, and show the correlations between the changes. It was found that modifying the measurement to increase the information tended to increase the disturbance, indicating a local trade-off relationship. However, because the correlation is imperfect, the information can be increased with decreasing the disturbance. We discuss a general scheme that improves the measurement to enhance the information gain while diminishing the disturbance.

Unlike the cases discussed in previous studies, the trade-off discussed in this paper concerns an infinitesimal change of a single-outcome process in a given measurement. The change is not finite, the outcome is not averaged, or the measurement is not optimized, so our trade-off is entirely local. Consequently, it gives a simple but fundamental relation in the quantum theory of measurements, thus broadening our perspective of quantum measurements.

The remainder of this paper is organized as follows. Section 2 reviews information and disturbance for a single outcome of a quantum measurement. Section 3 finds the steepest ascent and descent directions of the information and disturbance. In an exemplary case, Sec. 4 determines the local trade-off between information and disturbance on the basis of the steepest directions of both quantities. Section 5 correlates the information and disturbance by plotting their changes on a plane for various measurement modifications, obtaining a complete picture of the local trade-off. Section 6 discusses our

general measurement-improvement scheme that increases the information extraction while reducing the disturbance. Section 7 summarizes our results.

## 2 Preliminaries

To present a self-contained paper, we recall the information and disturbance for a single outcome of a quantum measurement [21]. Suppose that a quantum system is known to be in a pure state  $|\psi(a)\rangle$  with probability  $p(a)$ , where  $a = 1, \dots, N$ . To know the actual state of the system, we perform a quantum measurement on this system.

A quantum measurement is described by a set of measurement operators  $\{\hat{M}_m\}$  [22] satisfying

$$\sum_m \hat{M}_m^\dagger \hat{M}_m = \hat{I}, \quad (1)$$

where  $\hat{I}$  is the identity operator, and the index  $m$  denotes an outcome. For a system in state  $|\psi(a)\rangle$ , outcome  $m$  is obtained with probability

$$p(m|a) = \langle \psi(a) | \hat{M}_m^\dagger \hat{M}_m | \psi(a) \rangle. \quad (2)$$

After a measurement yielding outcome  $m$ , the system's state changes from  $|\psi(a)\rangle$  to

$$|\psi(m, a)\rangle = \frac{1}{\sqrt{p(m|a)}} \hat{M}_m |\psi(a)\rangle. \quad (3)$$

Note that this measurement does not change the system's state to a mixed state, because one operator retrieves one outcome. Such a non-classical measurement in the pure state is called an ideal measurement [23]. Here we demonstrate ideal measurements to clarify their quantum nature.

The outcome  $m$  provides information on the state of the system. More specifically, from the outcome  $m$ , one can naturally estimate the system's state as  $|\psi(a'_m)\rangle$ , where  $a'_m$  is  $a$  that maximizes  $p(m|a)$ , i.e.,  $p(m|a'_m) = \max_a p(m|a)$ . The quality of this estimate is determined by the estimation fidelity

$$G(m) = \sum_a p(a|m) |\langle \psi(a'_m) | \psi(a) \rangle|^2, \quad (4)$$

where we have used the conditional probability of the system's state being  $|\psi(a)\rangle$  given outcome  $m$ :

$$p(a|m) = \frac{p(m|a)p(a)}{p(m)}. \quad (5)$$

The total probability of  $m$  is

$$p(m) = \sum_a p(m|a) p(a). \quad (6)$$

The estimation fidelity  $G(m)$  provides a measure of the information provided by outcome  $m$ .

When a measurement yields outcome  $m$ , it changes the system's state from  $|\psi(a)\rangle$  to  $|\psi(m, a)\rangle$  given by Eq. (3). This disturbance of the system can be quantified by either the size or reversibility of the state change. The size of the state change can be evaluated by the operation fidelity

$$F(m) = \sum_a p(a|m) |\langle \psi(a) | \psi(m, a) \rangle|^2, \quad (7)$$

whereas the reversibility of the state change can be evaluated by performing reversing measurements [24, 25]. The reversing measurements are described by another set of measurement operators  $\{\hat{R}_\mu^{(m)}\}$  satisfying

$$\sum_\mu \hat{R}_\mu^{(m)\dagger} \hat{R}_\mu^{(m)} = \hat{I}, \quad (8)$$

where  $\hat{R}_{\mu_0}^{(m)} \propto \hat{M}_m^{-1}$  for a particular  $\mu = \mu_0$ . When the reversing measurement yields the preferred outcome  $\mu_0$ , the operator  $\hat{R}_{\mu_0}^{(m)}$  reverts the system's state from  $|\psi(m, a)\rangle$  to  $|\psi(a)\rangle$ . The maximum probability of this recovery, obtained from the best reversing measurement [26], is given by

$$R(m, a) = \frac{\inf_{|\psi\rangle} \langle \psi | \hat{M}_m^\dagger \hat{M}_m | \psi \rangle}{p(m|a)}. \quad (9)$$

Using this probability, the reversibility of the state change can be evaluated by the physical reversibility

$$R(m) = \sum_a p(a|m) R(m, a). \quad (10)$$

The operation fidelity  $F(m)$  and the physical reversibility  $R(m)$  quantify the disturbance caused by obtaining outcome  $m$ . Both measures decrease as the disturbance increases.

To explicitly calculate  $G(m)$ ,  $F(m)$ , and  $R(m)$ , we assume a completely unknown state of the system to be measured. That is, the set of possible

states  $\{|\psi(a)\rangle\}$  consists of all pure states of the system, and  $p(a)$  is uniform according to a normalized invariant measure over the pure states. In this case, the information and disturbance are functions of the singular values of  $\hat{M}_m$  [21]. Therefore, a measurement with outcome  $m$  can be conveniently expressed by the  $d$ -dimensional vector

$$\vec{\lambda}_m = (\lambda_{m1}, \lambda_{m2}, \dots, \lambda_{md}), \quad (11)$$

where  $d$  is the dimension of the Hilbert space of the system, and the components  $\{\lambda_{mi}\}$  are the singular values of  $\hat{M}_m$ . By definition, the singular values are not less than 0. Moreover, by Eq. (1), they cannot exceed 1. For simplicity, the singular values are sorted in the following descending order:

$$1 \geq \lambda_{m1} \geq \lambda_{m2} \geq \dots \geq \lambda_{md} \geq 0, \quad (12)$$

where  $\lambda_{m1} \neq 0$ . In terms of the singular values,  $G(m)$ ,  $F(m)$ , and  $R(m)$  are respectively written as [21]

$$G(m) = \frac{1}{d+1} \left( 1 + \frac{\lambda_{m1}^2}{\sigma_m^2} \right), \quad (13)$$

$$F(m) = \frac{1}{d+1} \left( 1 + \frac{\tau_m^2}{\sigma_m^2} \right), \quad (14)$$

$$R(m) = d \left( \frac{\lambda_{md}^2}{\sigma_m^2} \right), \quad (15)$$

where

$$\sigma_m^2 = \sum_{i=1}^d \lambda_{mi}^2, \quad \tau_m = \sum_{i=1}^d \lambda_{mi}. \quad (16)$$

Note that Eqs. (13)–(15) are invariant under rescaling of the singular values by a constant  $c$ ,

$$\vec{\lambda}_m \longrightarrow c\vec{\lambda}_m, \quad (17)$$

and under rearrangement of all singular values except  $\lambda_{m1}$  and  $\lambda_{md}$ . Note also that the maximum singular value  $\lambda_{m1}$  is used in Eq. (13) for  $G(m)$ , and the minimum singular value  $\lambda_{md}$  is used in Eq. (15) for  $R(m)$ .

To determine the allowed region of the information versus disturbance relationship, we plot all physically possible measurements on an information–disturbance plane. The allowed regions on the  $G(m)$  versus  $F(m)$  and  $G(m)$

versus  $R(m)$  planes are presented in Ref. [19]. The regions are formed by the lines and points corresponding to the measurements represented by the following vectors:

$$\vec{m}_{k,l}^{(d)}(\lambda) = c \left( \underbrace{1, 1, \dots, 1}_k, \underbrace{\lambda, \lambda, \dots, \lambda}_l, \underbrace{0, 0, \dots, 0}_{d-k-l} \right) \quad (18)$$

with  $0 \leq \lambda \leq 1$  and

$$\vec{p}_r^{(d)} = c \left( \underbrace{1, 1, \dots, 1}_r, \underbrace{0, 0, \dots, 0}_{d-r} \right). \quad (19)$$

The maximum  $G(m)$  and the minimum  $F(m)$  and  $R(m)$  are achieved by the projective measurement  $\vec{\lambda}_m = \vec{p}_1^{(d)}$ , whereas the minimum  $G(m)$  and the maximum  $F(m)$  and  $R(m)$  are achieved by the identity operation  $\vec{\lambda}_m = \vec{p}_d^{(d)}$ . The upper boundaries of the regions correspond to  $\vec{\lambda}_m = \vec{m}_{1,d-1}^{(d)}(\lambda)$  and the lower boundaries correspond to  $\vec{\lambda}_m = \vec{m}_{k,1}^{(d)}(\lambda)$  for  $k = 1, 2, \dots, d-1$ . As the upper boundaries are the upper bounds on  $G(m)$  for a given  $F(m)$  or  $R(m)$ , the measurements  $\vec{m}_{1,d-1}^{(d)}(\lambda)$  are optimal measurements. When an optimal measurement provides a large amount of information, it always causes a large disturbance, because the upper boundaries always have negative slopes [20].

### 3 Steepest Directions

Herein, we find the directions of steepest ascent and descent of  $G(m)$ ,  $F(m)$ , and  $R(m)$ . Under the conditions of Eq. (12), these directions are not necessarily parallel or antiparallel to the gradient vectors of  $G(m)$ ,  $F(m)$ , and  $R(m)$ . Consider modifying measurement  $\vec{\lambda}_m$  by an infinitesimal vector  $\vec{\epsilon}_m$  as

$$\vec{\lambda}'_m = \vec{\lambda}_m + \vec{\epsilon}_m. \quad (20)$$

After the vector modification  $\vec{\epsilon}_m$ ,  $\vec{\lambda}'_m$  must also satisfy the conditions of Eq. (12). This requirement is demanded only when  $\vec{\lambda}_m$  has some equal signs in Eq. (12), because  $\vec{\epsilon}_m$  is infinitesimal. In particular, considering the inequalities  $\lambda_{md} \geq 0$ ,  $\lambda_{m1} \geq \lambda_{mi}$ , and  $\lambda_{mi} \geq \lambda_{md}$  in Eq. (12),  $\vec{\epsilon}_m$  should satisfy

$$\vec{e}_d \cdot \vec{\epsilon}_m \geq 0 \quad \text{if } \lambda_{md} = 0, \quad (21)$$

$$(\vec{e}_1 - \vec{e}_i) \cdot \vec{\epsilon}_m \geq 0 \quad \text{if } \lambda_{m1} = \lambda_{mi}, \quad (22)$$

$$(\vec{e}_i - \vec{e}_d) \cdot \vec{\epsilon}_m \geq 0 \quad \text{if } \lambda_{mi} = \lambda_{md}, \quad (23)$$

where  $\vec{e}_i$  is the unit vector along the  $i$ th axis. The other inequalities in Eq. (12) can be ignored by rescaling and rearranging  $\vec{\lambda}'_m$ . Without changing  $G(m)$ ,  $F(m)$ , and  $R(m)$ ,  $\vec{\lambda}'_m$  is rescaled as Eq. (17) to satisfy  $\lambda'_{m1} \leq 1$  if  $\lambda'_{m1} > 1$ , and is rearranged to satisfy  $\lambda'_{mi} \geq \lambda'_{mj}$  if  $\lambda'_{mi} < \lambda'_{mj}$  ( $i < j$  with  $i \neq 1$  and  $j \neq d$ ). Therefore, from the conditional equations (21)–(23), we can find the steepest directions of  $G(m)$ ,  $F(m)$ , and  $R(m)$ .

The steepest-ascent direction of a function  $f$  is usually pointed by its gradient vector

$$\vec{\nabla} f = \left( \frac{\partial f}{\partial \lambda_{m1}}, \frac{\partial f}{\partial \lambda_{m2}}, \dots, \frac{\partial f}{\partial \lambda_{md}} \right). \quad (24)$$

From Eqs. (13)–(15), the gradient vectors of  $G(m)$ ,  $F(m)$ , and  $R(m)$  are respectively given by

$$\vec{\nabla} G(m) = \frac{2}{d+1} \left[ \frac{\lambda_{m1}}{\sigma_m^2} \left( \vec{e}_1 - \frac{\lambda_{m1}}{\sigma_m^2} \vec{\lambda}_m \right) \right], \quad (25)$$

$$\vec{\nabla} F(m) = \frac{2}{d+1} \left[ \frac{\tau_m}{\sigma_m^2} \left( \vec{l} - \frac{\tau_m}{\sigma_m^2} \vec{\lambda}_m \right) \right], \quad (26)$$

$$\vec{\nabla} R(m) = 2d \left[ \frac{\lambda_{md}}{\sigma_m^2} \left( \vec{e}_d - \frac{\lambda_{md}}{\sigma_m^2} \vec{\lambda}_m \right) \right], \quad (27)$$

where

$$\vec{l} = \sum_{i=1}^d \vec{e}_i. \quad (28)$$

Their respective magnitudes are given by

$$\left\| \vec{\nabla} G(m) \right\| = \frac{2}{d+1} \left( \frac{\lambda_{m1}}{\sigma_m^2} \sqrt{1 - \frac{\lambda_{m1}^2}{\sigma_m^2}} \right), \quad (29)$$

$$\left\| \vec{\nabla} F(m) \right\| = \frac{2}{d+1} \left( \frac{\tau_m}{\sigma_m^2} \sqrt{d - \frac{\tau_m^2}{\sigma_m^2}} \right), \quad (30)$$

$$\left\| \vec{\nabla} R(m) \right\| = 2d \left( \frac{\lambda_{md}}{\sigma_m^2} \sqrt{1 - \frac{\lambda_{md}^2}{\sigma_m^2}} \right) \quad (31)$$

and their respective unit vectors are

$$\vec{g}_m = \frac{\sigma_m}{\sqrt{\sigma_m^2 - \lambda_{m1}^2}} \left( \vec{e}_1 - \frac{\lambda_{m1}}{\sigma_m^2} \vec{\lambda}_m \right), \quad (32)$$

$$\vec{f}_m = \frac{\sigma_m}{\sqrt{d\sigma_m^2 - \tau_m^2}} \left( \vec{l} - \frac{\tau_m}{\sigma_m^2} \vec{\lambda}_m \right), \quad (33)$$

$$\vec{r}_m = \frac{\sigma_m}{\sqrt{\sigma_m^2 - \lambda_{md}^2}} \left( \vec{e}_d - \frac{\lambda_{md}}{\sigma_m^2} \vec{\lambda}_m \right). \quad (34)$$

Clearly,  $\vec{\epsilon}_m = \epsilon \vec{g}_m$  and  $\vec{\epsilon}_m = \epsilon \vec{f}_m$  with a positive infinitesimal  $\epsilon$  satisfy the conditions of Eqs. (21)–(23). Therefore, the unit vectors in the steepest-ascent directions of  $G(m)$  and  $F(m)$  are respectively given by

$$\vec{g}_m^{(+)} = \vec{g}_m, \quad (35)$$

$$\vec{f}_m^{(+)} = \vec{f}_m. \quad (36)$$

However,  $\vec{\epsilon}_m = \epsilon \vec{r}_m$  violates the condition of Eq. (23) if the minimum singular value is degenerate:

$$\lambda_{m(d-n_d+1)} = \lambda_{m(d-n_d+2)} = \cdots = \lambda_{md}, \quad (37)$$

where  $n_d$  is the degeneracy of the minimum singular value. In fact, if  $\lambda_{m(d-1)} = \lambda_{md}$  and  $i = d - 1$ , the condition of Eq. (23) is violated as

$$(\vec{e}_{d-1} - \vec{e}_d) \cdot \vec{r}_m = -\frac{\sigma_m}{\sqrt{\sigma_m^2 - \lambda_{md}^2}} < 0. \quad (38)$$

In this case,  $\vec{r}_m$  points from the boundary  $\lambda_{m(d-1)} = \lambda_{md}$  into the forbidden region  $\lambda_{m(d-1)} < \lambda_{md}$  (see Fig. 1). In the forbidden region,  $\vec{\lambda}'_m = \vec{\lambda}_m + \vec{\epsilon}_m$  should be rearranged such that  $\lambda'_{md}$  is smaller than the other singular values, meaning that  $R(m)$  decreases rather than increases. For example, when  $d = 3$  and  $\vec{\lambda}_m = (1, 1/2, 1/2)$ ,  $\vec{\epsilon}_m = \epsilon \vec{r}_m$  generates

$$\begin{aligned} \vec{\lambda}'_m &= \left( 1 - \frac{2\epsilon}{\sqrt{30}}, \frac{1}{2} - \frac{\epsilon}{\sqrt{30}}, \frac{1}{2} + \frac{5\epsilon}{\sqrt{30}} \right) \\ &\xrightarrow{\text{After rearranging}} \left( 1 - \frac{2\epsilon}{\sqrt{30}}, \frac{1}{2} + \frac{5\epsilon}{\sqrt{30}}, \frac{1}{2} - \frac{\epsilon}{\sqrt{30}} \right), \end{aligned} \quad (39)$$

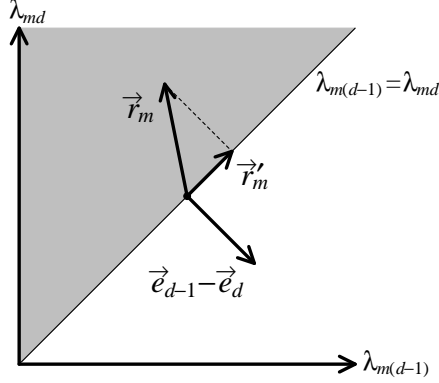


Figure 1: Gradient vector of  $R(m)$  on the boundary  $\lambda_{m(d-1)} = \lambda_{md}$

$R(m)$  decreases from  $1/2$  to  $(1/2) - (2\epsilon/\sqrt{30})$ . Hence,  $\vec{r}_m$  does not point in the direction of steepest ascent of  $R(m)$  if  $\lambda_{m(d-1)} = \lambda_{md}$ .

If  $\lambda_{m(d-1)} = \lambda_{md}$ , the direction of steepest ascent of  $R(m)$  is pointed by the vector  $\vec{r}'_m$  obtained by projecting  $\vec{r}_m$  onto the boundary, as shown in Fig. 1. Using the normal vector of the boundary,

$$\vec{n} = \frac{1}{\sqrt{2}} (\vec{e}_{d-1} - \vec{e}_d), \quad (40)$$

the projected vector is given by

$$\vec{r}'_m = \frac{\sigma_m}{\sqrt{\sigma_m^2 - \lambda_{md}^2}} \left( \frac{\vec{e}_{d-1} + \vec{e}_d}{2} - \frac{\lambda_{md}}{\sigma_m^2} \vec{\lambda}_m \right), \quad (41)$$

which satisfies the condition of Eq. (23) when  $i = d-1$ . However, if  $\lambda_{m(d-2)} = \lambda_{md}$ , the condition of Eq. (23) is violated when  $i = d-2$ . In that case,  $\vec{r}'_m$  is again projected onto the boundary  $\lambda_{m(d-2)} = \lambda_{md}$  using the normal vector

$$\vec{n}' = \sqrt{\frac{2}{3}} \left( \vec{e}_{d-2} - \frac{\vec{e}_{d-1} + \vec{e}_d}{2} \right). \quad (42)$$

In general, if the degeneracy of the minimum singular value is  $n_d$ ,  $\vec{r}_m$  should be projected  $(n_d - 1)$  times to satisfy the condition of Eq. (23) for all  $i$ . After normalizing the projected vector, the unit vector in the direction of steepest

ascent of  $R(m)$  is determined as

$$\vec{r}_m^{(+)} = \frac{\sqrt{n_d} \sigma_m}{\sqrt{\sigma_m^2 - n_d \lambda_{md}^2}} \left( \frac{1}{n_d} \vec{l}'_{n_d} - \frac{\lambda_{md}}{\sigma_m^2} \vec{\lambda}_m \right), \quad (43)$$

where

$$\vec{l}'_n = \sum_{i=d-n+1}^d \vec{e}_i. \quad (44)$$

The angle  $\theta_r$  between  $\vec{r}_m^{(+)}$  and  $\vec{r}_m$  is given by

$$\cos \theta_r = \vec{r}_m^{(+)} \cdot \vec{r}_m = \sqrt{\frac{\sigma_m^2 - n_d \lambda_{md}^2}{n_d (\sigma_m^2 - \lambda_{md}^2)}}. \quad (45)$$

Similarly, the steepest-descent direction of a function  $f$  is not necessarily pointed by  $-\vec{\nabla} f$  under the conditions of Eqs. (21)–(23). For example,  $\vec{\epsilon}_m = -\epsilon \vec{g}_m$  violates the condition of Eq. (22) if the maximum singular value is degenerate:

$$\lambda_{m1} = \lambda_{m2} = \dots = \lambda_{mn_1}, \quad (46)$$

where  $n_1$  is the degeneracy of the maximum singular value. By projecting and normalizing  $-\vec{g}_m$ , the unit vector in the steepest-descent direction of  $G(m)$  is given by

$$\vec{g}_m^{(-)} = -\frac{\sqrt{n_1} \sigma_m}{\sqrt{\sigma_m^2 - n_1 \lambda_{m1}^2}} \left( \frac{1}{n_1} \vec{l}_{n_1} - \frac{\lambda_{m1}}{\sigma_m^2} \vec{\lambda}_m \right), \quad (47)$$

where

$$\vec{l}_n = \sum_{i=1}^n \vec{e}_i. \quad (48)$$

The angle  $\theta_g$  between  $\vec{g}_m^{(-)}$  and  $-\vec{g}_m$  is given by

$$\cos \theta_g = -\vec{g}_m^{(-)} \cdot \vec{g}_m = \sqrt{\frac{\sigma_m^2 - n_1 \lambda_{m1}^2}{n_1 (\sigma_m^2 - \lambda_{m1}^2)}}. \quad (49)$$

Moreover,  $\vec{\epsilon}_m = -\epsilon \vec{f}_m$  violates the condition of Eq. (21) if some singular values are 0:

$$\lambda_{m(d-n_0+1)} = \lambda_{m(d-n_0+2)} = \dots = \lambda_{md} = 0, \quad (50)$$

where  $n_0$  is the degeneracy of the singular value 0. Of course,  $n_0 = 0$  if  $\lambda_{md} \neq 0$ , and  $n_0 = n_d$  if  $\lambda_{md} = 0$ . By projecting and normalizing  $-\vec{f}_m$ , the unit vector in the steepest-descent direction of  $F(m)$  is given by

$$\vec{f}_m^{(-)} = -\frac{\sigma_m}{\sqrt{(d-n_0)\sigma_m^2 - \tau_m^2}} \left( \vec{l}_{d-n_0} - \frac{\tau_m}{\sigma_m^2} \vec{\lambda}_m \right). \quad (51)$$

The angle  $\theta_f$  between  $\vec{f}_m^{(-)}$  and  $-\vec{f}_m$  is given by

$$\cos \theta_f = -\vec{f}_m^{(-)} \cdot \vec{f}_m = \sqrt{\frac{(d-n_0)\sigma_m^2 - \tau_m^2}{d\sigma_m^2 - \tau_m^2}}. \quad (52)$$

Finally,  $\vec{e}_m = -\epsilon \vec{r}_m$  violates the condition of Eq. (21) if  $\lambda_{md} = 0$ , because  $-\vec{r}_m = -\vec{e}_d$ . As the projected vector of  $-\vec{e}_d$  on the boundary  $\lambda_{md} = 0$  is the zero vector  $\vec{0}$ , the unit vector in the steepest-descent direction of  $R(m)$  is given by

$$\vec{r}_m^{(-)} = -\delta_{n_0,0} \vec{r}_m, \quad (53)$$

because  $n_0 \neq 0$  if  $\lambda_{md} = 0$ .

Summarizing the above, for a measurement  $\vec{\lambda}_m$ , the directions of steepest ascent and descent of  $G(m)$  are given by Eqs. (35) and (47), respectively, where Eq. (35) uses the unit gradient vector in Eq. (32). Meanwhile, the directions of steepest ascent and descent of  $F(m)$  are given by Eqs. (36) and (51), respectively, where Eq. (36) uses the unit gradient vector in Eq. (33). Finally, the directions of steepest ascent and descent of  $R(m)$  are given by Eqs. (43) and (53), respectively, where Eq. (53) uses the unit gradient vector in Eq. (34). All of these vectors are orthogonal to  $\vec{\lambda}_m$ :

$$\vec{\lambda}_m \cdot \vec{g}_m = \vec{\lambda}_m \cdot \vec{g}_m^{(\pm)} = 0, \quad (54)$$

$$\vec{\lambda}_m \cdot \vec{f}_m = \vec{\lambda}_m \cdot \vec{f}_m^{(\pm)} = 0, \quad (55)$$

$$\vec{\lambda}_m \cdot \vec{r}_m = \vec{\lambda}_m \cdot \vec{r}_m^{(\pm)} = 0. \quad (56)$$

This is because  $G(m)$ ,  $F(m)$ , and  $R(m)$  are invariant under the rescaling operation in Eq. (17).

When a zero vector is normalized, the above equations give  $\vec{0}/0$  or  $0/0$ . For example, when  $\vec{\lambda}_m = \vec{p}_1^{(d)}$ , Eq. (32) gives  $\vec{g}_m = \vec{0}/0$  because  $\vec{\nabla}G(m) = \vec{0}$  from Eq. (25). Note that the limit of  $\vec{g}_m$  as  $\vec{\lambda}_m \rightarrow \vec{p}_1^{(d)}$  does not exist. In

such cases, it is simple and proper to assume that

$$\frac{\vec{0}}{0} = \vec{0}, \quad \frac{0}{0} = 0. \quad (57)$$

Assuming Eq. (57), we obtain

$$\vec{g}_m = \vec{g}_m^{(+)} = \vec{0}, \quad \cos \theta_g = 0 \quad \text{at } \vec{\lambda}_m = \vec{p}_1^{(d)}, \quad (58)$$

$$\vec{f}_m = \vec{f}_m^{(+)} = \vec{r}_m^{(+)} = \vec{0}, \quad \cos \theta_f = 0 \quad \text{at } \vec{\lambda}_m = \vec{p}_d^{(d)}, \quad (59)$$

$$\vec{g}_m^{(-)} = \vec{f}_m^{(-)} = \vec{0} \quad \text{at } \vec{\lambda}_m = \vec{p}_r^{(d)} \quad (60)$$

with  $r = 1, 2, \dots, d$ .

## 4 Local Trade-off

We now derive the local trade-off between the information and disturbance in terms of their steepest directions. When a measurement is slightly modified to increase the amount of obtained information, it usually increases the disturbance in the system. This local trade-off depends on the angle between the steepest directions of the information and disturbance. On the basis of this angle, we discuss the local trade-off in two information–disturbance pairs:  $G(m)$  versus  $F(m)$  and  $G(m)$  versus  $R(m)$ .

We first consider  $G(m)$  and  $F(m)$  as an information–disturbance pair. The angle between the steepest-ascent directions of  $G(m)$  and  $F(m)$  is represented by the dot product

$$C_{GF}^{(++)} = \vec{g}_m^{(+)} \cdot \vec{f}_m^{(+)} \quad (61)$$

Because the two vectors are normalized, the dot product is simply the cosine of the angle. Inserting Eqs. (32) and (33) into Eqs. (35) and (36), respectively, its value is determined as

$$C_{GF}^{(++)} = -\frac{\tau_m \lambda_{m1} - \sigma_m^2}{\sqrt{(\sigma_m^2 - \lambda_{m1}^2)(d\sigma_m^2 - \tau_m^2)}} \leq 0, \quad (62)$$

which is a function of  $\vec{\lambda}_m$ . Note that by Eq. (57),  $C_{GF}^{(++)} = 0$  if  $\vec{\lambda}_m = \vec{p}_1^{(d)}$  or  $\vec{\lambda}_m = \vec{p}_d^{(d)}$ . The last inequality of Eq. (62) is proven as

$$\tau_m \lambda_{m1} - \sigma_m^2 = \sum_i \lambda_{mi} (\lambda_{m1} - \lambda_{mi}) \geq 0. \quad (63)$$

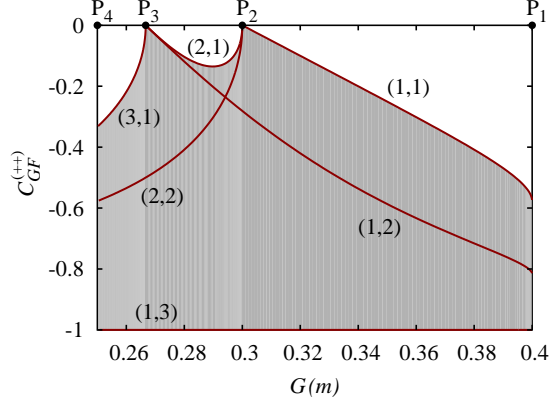


Figure 2: Possible range of  $C_{GF}^{(++)}$  as a function of  $G(m)$  in  $d = 4$

As  $C_{GF}^{(++)} \leq 0$ , the angle between  $\vec{g}_m^{(+)}$  and  $\vec{f}_m^{(+)}$  is either right or obtuse. The maximum value  $C_{GF}^{(++)} = 0$  is achieved at  $\vec{\lambda}_m = \vec{p}_r^{(d)}$ , whereas the minimum value  $C_{GF}^{(++)} = -1$  is achieved by the optimal measurements  $\vec{\lambda}_m = \vec{m}_{1,d-1}^{(d)}(\lambda)$ .

Figure 2 shows the possible range of  $C_{GF}^{(++)}$  as a function of  $G(m)$  in  $d = 4$ . The possible range is determined similarly to Appendix A of Ref. [19]. In this figure, the point  $P_r$  denotes  $\vec{p}_r^{(d)}$  and the line  $(k, l)$  denotes  $\vec{m}_{k,l}^{(d)}(\lambda)$  as  $0 < \lambda < 1$ . Interestingly,  $C_{GF}^{(++)}$  cannot have unique limits as  $\vec{\lambda}_m \rightarrow \vec{p}_1^{(d)}$  and  $\vec{\lambda}_m \rightarrow \vec{p}_d^{(d)}$ , where  $C_{GF}^{(++)} = 0$  by Eqs. (58) and (59). For example, although both  $\vec{m}_{3,1}^{(4)}(1 - \delta)$  and  $\vec{m}_{2,2}^{(4)}(1 - \delta)$  become  $\vec{p}_4^{(4)}$  when  $G(m) = 1/4$  at  $\delta = 0$ , they give different limits of  $C_{GF}^{(++)}$  as  $\delta \rightarrow 0$ , as shown by lines (3, 1) and (2, 2) in Fig. 2.

Using  $C_{GF}^{(++)}$ , we now discuss the local trade-off between  $G(m)$  and  $F(m)$  for measurement  $\vec{\lambda}_m$ . When  $\vec{\lambda}_m$  is modified by  $\vec{\epsilon}_m$  as in Eq. (20),  $G(m)$  and  $F(m)$  respectively change as follows:

$$\Delta G(m) = \vec{\epsilon}_m \cdot \vec{\nabla} G(m) = (\vec{\epsilon}_m \cdot \vec{g}_m) \left\| \vec{\nabla} G(m) \right\|, \quad (64)$$

$$\Delta F(m) = \vec{\epsilon}_m \cdot \vec{\nabla} F(m) = (\vec{\epsilon}_m \cdot \vec{f}_m) \left\| \vec{\nabla} F(m) \right\|. \quad (65)$$

The angle between  $\vec{g}_m$  and  $\vec{f}_m$  cannot be acute because its cosine is

$$C_{GF} = \vec{g}_m \cdot \vec{f}_m = C_{GF}^{(++)} \leq 0. \quad (66)$$

Thus, when the modification  $\vec{\epsilon}_m$  gives  $\Delta G(m) > 0$ , the local trade-off usually gives  $\Delta F(m) < 0$ . For example, when set to  $\epsilon \vec{g}_m^{(+)}$ , the modification increases  $G(m)$  as far as possible. In this case,  $G(m)$  increases by

$$[\Delta G(m)]_{\max} = \epsilon \left\| \vec{\nabla} G(m) \right\| \geq 0. \quad (67)$$

However, under the trade-off relationship,  $F(m)$  decreases as

$$\Delta F(m) = C_{GF}^{(++)} [\Delta F(m)]_{\max} \leq 0, \quad (68)$$

where

$$[\Delta F(m)]_{\max} = \epsilon \left\| \vec{\nabla} F(m) \right\| \geq 0 \quad (69)$$

is  $\Delta F(m)$  when  $F(m)$  is increased as far as possible by  $\vec{\epsilon}_m = \epsilon \vec{f}_m^{(+)}$ . A similar relation holds after interchanging the roles of  $G(m)$  and  $F(m)$ . This example demonstrates the local trade-off between  $G(m)$  and  $F(m)$ , which is quantified by  $C_{GF}^{(++)}$ .

We next consider  $G(m)$  and  $R(m)$  as an information–disturbance pair. Unlike the case of  $G(m)$  versus  $F(m)$ ,  $\vec{r}_m^{(+)}$  is not equal to  $\vec{r}_m$  if  $n_d > 1$  under the condition of Eq. (23) (see Eqs. (34) and (43)). The cosine of the angle between  $\vec{g}_m^{(+)}$  and  $\vec{r}_m^{(+)}$  is given by

$$C_{GR}^{(++)} = \vec{g}_m^{(+)} \cdot \vec{r}_m^{(+)} \quad (70)$$

Using Eqs. (35) and (43), this cosine is calculated as

$$C_{GR}^{(++)} = -\frac{\sqrt{n_d} \lambda_{m1} \lambda_{md} (1 - \delta_{n_d, d})}{\sqrt{(\sigma_m^2 - \lambda_{m1}^2) (\sigma_m^2 - n_d \lambda_{md}^2)}} \leq 0, \quad (71)$$

which is a function of  $\vec{\lambda}_m$ . Note that by Eq. (57),  $C_{GR}^{(++)} = 0$  if  $\vec{\lambda}_m = \vec{p}_1^{(d)}$  or  $\vec{\lambda}_m = \vec{p}_d^{(d)}$ , where  $n_d = d$  when  $\vec{\lambda}_m = \vec{p}_d^{(d)}$ . As obtained for  $G(m)$  versus  $F(m)$ , the angle between  $\vec{g}_m^{(+)}$  and  $\vec{r}_m^{(+)}$  is either right or obtuse. The maximum value  $C_{GR}^{(++)} = 0$  is achieved at  $\lambda_{md} = 0$  or  $\vec{\lambda}_m = \vec{p}_d^{(d)}$ , whereas the minimum value  $C_{GR}^{(++)} = -1$  is achieved by the optimal measurements  $\vec{\lambda}_m = \vec{m}_{1, d-1}^{(d)}(\lambda)$  using  $n_d = d - 1$ .

Figure 3 shows the possible range of  $C_{GR}^{(++)}$  as a function of  $G(m)$  in  $d = 4$ . The dotted line  $(1, d - 1)_n$  denotes

$$\vec{\lambda}_m = c \left( 1, \underbrace{\lambda + \delta, \lambda + \delta, \dots, \lambda + \delta}_{d-n-1}, \underbrace{\lambda, \lambda, \dots, \lambda}_n \right), \quad (72)$$

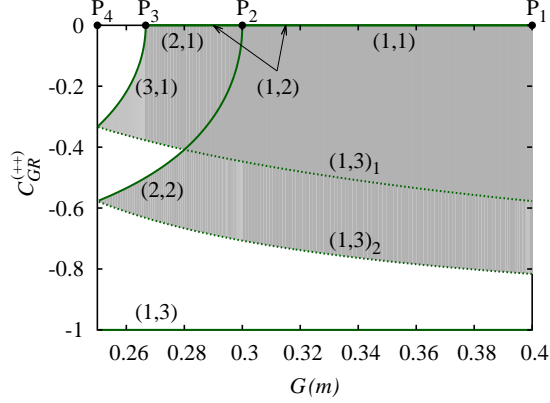


Figure 3: Possible range of  $C_{GR}^{(++)}$  as a function of  $G(m)$  in  $d = 4$

with  $0 < \lambda < 1$  using  $n_d = n$  but  $\delta \rightarrow 0$ . The points on this line are excluded from the possible region because  $C_{GR}^{(++)}$  jumps to  $-1$  when  $n_d = d - 1$  at  $\delta = 0$ . Apart from the straight line  $C_{GR}^{(++)} = -1$  defined by the optimal measurements, the region is divided into  $d - 2$  overlapping subregions. The  $n$ th subregion, enclosed by the lines  $(d - n, n)$ ,  $(1, d - n - 1)$ , and  $(1, d - 1)_n$ , is generated by measurements having  $n_d = n$ . Similarly to the case of  $G(m)$  versus  $F(m)$ ,  $C_{GR}^{(++)}$  cannot have unique limits as  $\vec{\lambda}_m \rightarrow \vec{p}_1^{(d)}$  and  $\vec{\lambda}_m \rightarrow \vec{p}_d^{(d)}$ , where  $C_{GR}^{(++)} = 0$  by Eqs. (58) and (59).

In contrast, the cosine of the angle between  $\vec{g}_m$  and  $\vec{r}_m$  is given by

$$C_{GR} = \vec{g}_m \cdot \vec{r}_m. \quad (73)$$

From Eqs. (32) and (34), this cosine is explicitly given by

$$C_{GR} = -\frac{\lambda_{m1}\lambda_{md}}{\sqrt{(\sigma_m^2 - \lambda_{m1}^2)(\sigma_m^2 - \lambda_{md}^2)}} \leq 0. \quad (74)$$

The possible region of  $C_{GR}$  equals the first subregion of  $C_{GR}^{(++)}$  plus the points on the line  $(1, d - 1)_1$ , because in the  $C_{GR}$  calculation,  $n_d = 1$  for any  $\vec{\lambda}_m$ . Thus,  $C_{GR} = -1$  cannot be achieved by any measurement. Although the optimal measurements  $\vec{m}_{1,d-1}^{(d)}(\lambda)$  correspond to the lower boundary  $(1, d - 1)_1$  of the possible region of  $C_{GR}$ , they give

$$C_{GR} = -\frac{1}{\sqrt{(d-1)[1+(d-2)\lambda^2]}} > -1 \quad (75)$$

depending on  $\lambda$ . From Eq. (45),  $C_{GR}^{(++)}$  and  $C_{GR}$  are related as

$$C_{GR} = C_{GR}^{(++)} \cos \theta_r \quad (76)$$

if  $\vec{\lambda}_m \neq \vec{p}_d^{(d)}$ . If  $\vec{\lambda}_m = \vec{p}_d^{(d)}$ ,  $C_{GR}^{(++)} = \cos \theta_r = 0$  but  $C_{GR} = -1/(d-1)$ .

Using  $C_{GR}^{(++)}$  with  $C_{GR}$ , we discuss the local trade-off between  $G(m)$  and  $R(m)$  for measurement  $\vec{\lambda}_m$ . When  $\vec{\lambda}_m$  is modified by  $\vec{\epsilon}_m$ ,  $R(m)$  changes by

$$\Delta R(m) = \vec{\epsilon}_m \cdot \vec{\nabla} R(m) = (\vec{\epsilon}_m \cdot \vec{r}_m) \left\| \vec{\nabla} R(m) \right\|. \quad (77)$$

The angle between  $\vec{g}_m$  and  $\vec{r}_m$  cannot be acute because  $C_{GR} \leq 0$ . Thus, when the modification  $\vec{\epsilon}_m$  gives  $\Delta G(m) > 0$ , the local trade-off usually gives  $\Delta R(m) < 0$ . For example, when  $\vec{\epsilon}_m$  is set to  $\epsilon \vec{g}_m^{(+)}$  for  $\vec{\lambda}_m \neq \vec{p}_d^{(d)}$ ,  $G(m)$  is increased as far as possible but  $R(m)$  decreases as

$$\Delta R(m) = C_{GR}^{(++)} [\Delta R(m)]_{\max} \leq 0 \quad (78)$$

by Eq. (76), where

$$[\Delta R(m)]_{\max} = \epsilon \left\| \vec{\nabla} R(m) \right\| \cos \theta_r \geq 0. \quad (79)$$

When  $R(m)$  is increased as far as possible by  $\vec{\epsilon}_m = \epsilon \vec{r}_m^{(+)}$  (not by  $\vec{\epsilon}_m = \epsilon \vec{r}_m$ ), Eq. (79) becomes  $\Delta R(m)$ . Note that  $\vec{\epsilon}_m = \epsilon \vec{r}_m$  is forbidden under the condition of Eq. (23). A similar relation holds after interchanging the roles of  $G(m)$  and  $R(m)$ . This example demonstrates the local trade-off between  $G(m)$  and  $R(m)$ , which is quantified by  $C_{GR}^{(++)}$  rather than  $C_{GR}$ .

## 5 Correlations

To completely understand the local trade-off, we correlate the information change with the disturbance change by plotting the two changes on a plane for various measurement modifications. The points to be plotted are distributed in a region enclosed by four elliptical arcs. Herein, we show that these four arcs are characterized by four different angles between the steepest directions of the information and disturbance.

The changes in the  $G(m)$  versus  $F(m)$  information–disturbance pair of a measurement  $\vec{\lambda}_m$  after a modification  $\vec{\epsilon}_m$  (Eqs. (64) and (65), respectively)

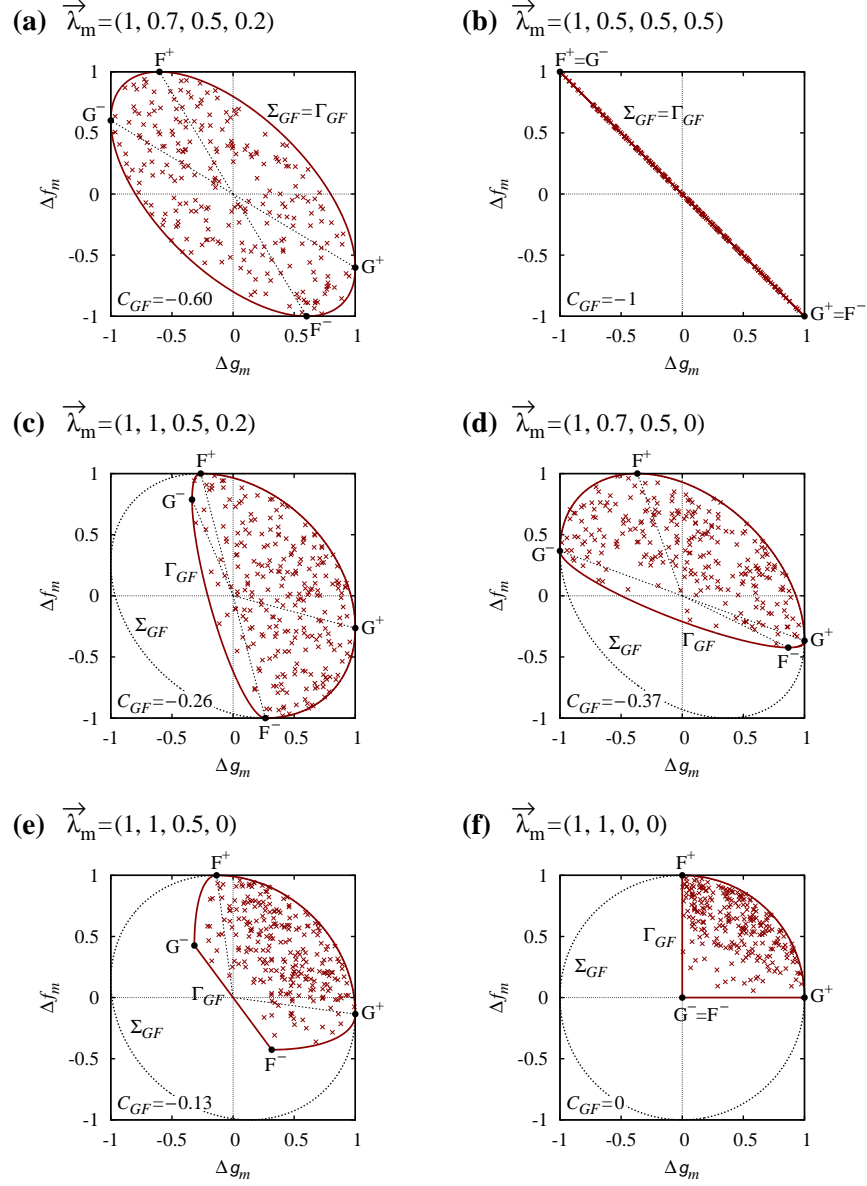


Figure 4: Correlations between  $\Delta g_m$  and  $\Delta f_m$  for six different measurements in  $d = 4$

are normalized as

$$\Delta g_m = \frac{\Delta G(m)}{\|\vec{\epsilon}_m\| \|\vec{\nabla} G(m)\|} = \frac{\vec{\epsilon}_m}{\|\vec{\epsilon}_m\|} \cdot \vec{g}_m, \quad (80)$$

$$\Delta f_m = \frac{\Delta F(m)}{\|\vec{\epsilon}_m\| \|\vec{\nabla} F(m)\|} = \frac{\vec{\epsilon}_m}{\|\vec{\epsilon}_m\|} \cdot \vec{f}_m. \quad (81)$$

The correlations between  $\Delta g_m$  and  $\Delta f_m$  are clarified in Fig. 4. The points in this figure were generated after 250 random modifications of six measurements in  $d = 4$  satisfying the conditions of Eqs. (21) and (22) with  $\|\vec{\epsilon}_m\| = 0.01$ . Here, the condition of Eq. (23) is not imposed on  $\vec{\epsilon}_m$  because  $R(m)$  is not involved. Provided that  $R(m)$  is excluded, the inequality  $\lambda_{mi} \geq \lambda_{md}$  in Eq. (12) can be removed by rearranging  $\vec{\lambda}'_m$  such that  $\lambda'_{mi} \geq \lambda'_{md}$  if  $\lambda'_{mi} < \lambda'_{md}$ , without changing  $G(m)$  and  $F(m)$ .

All plotted points lie inside the ellipse  $\Sigma_{GF}$  generated by

$$\Sigma_{GF} : \quad \vec{\epsilon}_m = \epsilon \vec{g}_m \cos \phi + \epsilon \vec{f}_m \sin \phi, \quad (82)$$

where  $0 \leq \phi < 2\pi$ . The ellipse  $\Sigma_{GF}$  is described by

$$(\Delta g_m)^2 + (\Delta f_m)^2 - 2C_{GF} \Delta g_m \Delta f_m = 1 - (C_{GF})^2, \quad (83)$$

with a tilt angle of  $-45^\circ$ . The shape of  $\Sigma_{GF}$  is characterized by  $C_{GF}$ , being circular when  $C_{GF} = 0$ , linear (with slope  $-1$ ) when  $C_{GF} = -1$ , and elliptical (as described above) otherwise. In Fig. 4, points  $G^\pm$  and  $F^\pm$  correspond to  $\vec{\epsilon}_m = \epsilon \vec{g}_m^{(\pm)}$  and  $\vec{\epsilon}_m = \epsilon \vec{f}_m^{(\pm)}$ , respectively. Their coordinates are given by

$$\begin{aligned} G^+ &: \quad \left( 1 - \delta_{n_0, (d-1)}, C_{GF}^{(++)} \right), \\ F^+ &: \quad \left( C_{GF}^{(++)}, 1 - \delta_{n_1, d} \right), \\ G^- &: \quad \left( -\cos \theta_g, C_{GF}^{(-+)} \right), \\ F^- &: \quad \left( C_{GF}^{(+-)}, -\cos \theta_f \right), \end{aligned} \quad (84)$$

where  $C_{GF}^{(-+)} = \vec{g}_m^{(-)} \cdot \vec{f}_m^{(+)}$  and  $C_{GF}^{(+-)} = \vec{g}_m^{(+)} \cdot \vec{f}_m^{(-)}$  are respectively given by

$$C_{GF}^{(-+)} = \frac{\sqrt{n_1} (\tau_m \lambda_{m1} - \sigma_m^2)}{\sqrt{(\sigma_m^2 - n_1 \lambda_{m1}^2) (d\sigma_m^2 - \tau_m^2)}} \geq 0, \quad (85)$$

$$C_{GF}^{(+-)} = \frac{\tau_m \lambda_{m1} - \sigma_m^2}{\sqrt{(\sigma_m^2 - \lambda_{m1}^2) [(d - n_0) \sigma_m^2 - \tau_m^2]}} \geq 0. \quad (86)$$

Note that by Eq. (58),  $\vec{g}_m^{(+)} \cdot \vec{g}_m = 0$  when  $n_0 = d - 1$  and by Eq. (59),  $\vec{f}_m^{(+)} \cdot \vec{f}_m = 0$  when  $n_1 = d$ . The point  $G^+$  is obtained by Eqs. (67) and (68).

If  $n_1 = 1$  and  $n_0 = 0$ , the plotted points are distributed through the whole region inside  $\Sigma_{GF}$  and the four points  $G^\pm$  and  $F^\pm$  are on  $\Sigma_{GF}$ , as shown for the measurement  $\vec{\lambda}_m = (1, 0.7, 0.5, 0.2)$  in Fig. 4(a). The tilt of  $\Sigma_{GF}$  indicates that  $\Delta g_m$  and  $\Delta f_m$  are negatively correlated. In this case,  $C_{GF}$  can be related to the Pearson correlation coefficient using isotropic modifications in the  $d$ -dimensional space. When  $\vec{\epsilon}_m^{(n)}$  are normalized to  $\epsilon$  for  $n = 1, 2, \dots, N_p$ , they are assumed to be isotropic as

$$\frac{1}{N_p} \sum_n \epsilon_{mi}^{(n)} = 0, \quad (87)$$

$$\frac{1}{N_p} \sum_n \epsilon_{mi}^{(n)} \epsilon_{mj}^{(n)} = \frac{\epsilon^2}{d} \delta_{i,j}, \quad (88)$$

where  $\epsilon_{mi}^{(n)}$  is the  $i$ th component of  $\vec{\epsilon}_m^{(n)}$ . The Pearson correlation coefficient of the points obtained using modifications  $\vec{\epsilon}_m^{(n)}$  equals  $C_{GF}$ . The optimal measurements  $\vec{\lambda}_m = \vec{m}_{1,d-1}^{(d)}(\lambda)$  yield a perfect negative correlation  $C_{GF} = -1$ . Figure 4(b) shows such a case for  $\vec{\lambda}_m = (1, 0.5, 0.5, 0.5)$ , where  $\Sigma_{GF}$  is a straight line. Conversely, the non-correlated case  $C_{GF} = 0$  is prohibited when  $n_1 = 1$  and  $n_0 = 0$ .

Under the conditions of Eqs. (21) and (22), if  $n_1 > 1$  or  $n_0 > 0$ , the plotted points distribute only in a subregion of the region enclosed by  $\Sigma_{GF}$ . These cases are presented in Fig. 4(c) for  $\vec{\lambda}_m = (1, 1, 0.5, 0.2)$  with  $n_1 = 2$ , Fig. 4(d) for  $\vec{\lambda}_m = (1, 0.7, 0.5, 0)$  with  $n_0 = 1$ , and Fig. 4(e) for  $\vec{\lambda}_m = (1, 1, 0.5, 0)$  with  $n_1 = 2$  and  $n_0 = 1$ . Although  $G^+$  and  $F^+$  are always on  $\Sigma_{GF}$ ,  $G^-$  is not on  $\Sigma_{GF}$  if  $n_1 > 1$ , and  $F^-$  is not on  $\Sigma_{GF}$  if  $n_0 > 0$ . The boundary  $\Gamma_{GF}$  of the subregion consists of four curves connecting the four points  $G^+$ ,  $F^+$ ,  $G^-$ , and  $F^-$ . These curves are generated as follows:

$$\begin{aligned} G^+ \rightarrow F^+ : \quad \vec{\epsilon}_m &= \epsilon \vec{g}_m^{(+)} \cos \phi + \epsilon \vec{f}_m^{(+)} \sin \phi, \\ F^+ \rightarrow G^- : \quad \vec{\epsilon}_m &= \epsilon \vec{g}_m^{(-)} \sin \phi + \epsilon \vec{f}_m^{(+)} \cos \phi, \\ G^- \rightarrow F^- : \quad \vec{\epsilon}_m &= \epsilon \vec{g}_m^{(-)} \cos \phi + \epsilon \vec{f}_m^{(-)} \sin \phi, \\ F^- \rightarrow G^+ : \quad \vec{\epsilon}_m &= \epsilon \vec{g}_m^{(+)} \sin \phi + \epsilon \vec{f}_m^{(-)} \cos \phi, \end{aligned} \quad (89)$$

where  $0 \leq \phi < \pi/2$ .

The shape of  $\Gamma_{GF}$  is characterized by four angles between the steepest directions:  $C_{GF}^{(++)}$ ,  $C_{GF}^{(-+)}$ ,  $C_{GF}^{(+-)}$ , and  $C_{GF}^{(--)} = \vec{g}_m^{(-)} \cdot \vec{f}_m^{(-)}$ . The latter is given by

$$C_{GF}^{(--)} = -\frac{\sqrt{n_1}(\tau_m \lambda_{m1} - \sigma_m^2)}{\sqrt{(\sigma_m^2 - n_1 \lambda_{m1}^2)[(d - n_0)\sigma_m^2 - \tau_m^2]}} \leq 0. \quad (90)$$

These terms are related as follows:

$$\begin{aligned} C_{GF}^{(++)} &= -C_{GF}^{(-+)} \cos \theta_g = C_{GF}^{(--)} \cos \theta_g \cos \theta_f \\ &= -C_{GF}^{(+-)} \cos \theta_f = C_{GF}. \end{aligned} \quad (91)$$

Between  $G^+$  and  $F^+$ , the boundary  $\Gamma_{GF}$  is an arc of the ellipse  $\Sigma_{GF}$  given by Eq. (83) with  $C_{GF} = C_{GF}^{(++)}$ , but between  $F^+$  and  $G^-$ , it is an arc of the ellipse described by

$$(\Delta g'_m)^2 + (\Delta f_m)^2 + 2C_{GF}^{(-+)} \Delta g'_m \Delta f_m = 1 - [C_{GF}^{(-+)}]^2, \quad (92)$$

where we have used  $\Delta g'_m = \Delta g_m / \cos \theta_g$  and Eq. (91). This ellipse is obtained by horizontally compressing the ellipse  $\Sigma_{GF}$  by a factor of  $1/\cos \theta_g$  and replacing  $C_{GF}$  with  $-C_{GF}^{(-+)} = C_{GF} / \cos \theta_g$ . When  $C_{GF}^{(-+)} = 0$ , this ellipse is untilted with axes  $\cos \theta_g$  and 1, but when  $C_{GF}^{(-+)} = 1$ , it collapses to a straight line with slope  $-1/\cos \theta_g$  (i.e.,  $F^+$  coincides with  $G^-$ ). Similarly,  $\Gamma_{GF}$  is an arc of the ellipse described by

$$(\Delta g'_m)^2 + (\Delta f'_m)^2 - 2C_{GF}^{(--)} \Delta g'_m \Delta f'_m = 1 - [C_{GF}^{(--)}]^2 \quad (93)$$

with  $\Delta f'_m = \Delta f_m / \cos \theta_f$  between  $G^-$  and  $F^-$ , and is an arc of the ellipse described by

$$(\Delta g_m)^2 + (\Delta f'_m)^2 + 2C_{GF}^{(+-)} \Delta g_m \Delta f'_m = 1 - [C_{GF}^{(+-)}]^2 \quad (94)$$

between  $F^-$  and  $G^+$ .

Therefore, we can naturally represent the correlation between  $\Delta g_m$  and  $\Delta f_m$  by the four coefficients  $C_{GF}^{(++)}$ ,  $-C_{GF}^{(-+)}$ ,  $C_{GF}^{(--)}$ , and  $-C_{GF}^{(+-)}$ . For example, in Fig. 4(c),  $C_{GF}^{(++)} = -C_{GF}^{(-+)} = -0.26$  and  $C_{GF}^{(--)} = -C_{GF}^{(+-)} = -0.79$ , denoting that  $\Gamma_{GF}$  is flatter in the left region of the straight line between  $F^+$  and  $F^-$  than in the right region. In Fig. 4(d),  $C_{GF}^{(++)} = -C_{GF}^{(-+)} = -0.37$  and  $C_{GF}^{(--)} = -C_{GF}^{(+-)} = -0.87$ , denoting that  $\Gamma_{GF}$  is flatter in the lower region of

the straight line between  $G^+$  and  $G^-$  than in the upper region. In Fig. 4(e),  $\Gamma_{GF}$  is linear between  $G^-$  and  $F^-$  because  $C_{GF}^{(--)} = -1$ . If  $n_1 = 1$  and  $n_0 = 0$ , the four coefficients are equal as shown in Fig. 4(a).

Unfortunately, the case of  $C_{GF} = 0$  is anomalous. This case occurs when  $\vec{\lambda}_m = \vec{p}_r^{(d)}$  with  $r = 1, 2, \dots, d$ , for which  $C_{GF}^{(\pm\pm)} = 0$  with  $n_1 = r$  and  $n_0 = d - r$ . If  $r \neq 1$  and  $r \neq d$ ,  $\Gamma_{GF}$  is the first-quadrant quarter of the circle  $\Sigma_{GF}$  (see Fig. 4(f) for  $\vec{\lambda}_m = (1, 1, 0, 0)$ ) although  $C_{GF}^{(-+)} = C_{GF}^{(--)} = C_{GF}^{(+-)} = 0$ , because  $\cos \theta_g = \cos \theta_f = 0$  by Eq. (60). Conversely, if  $r = 1$  or  $r = d$ ,  $\Sigma_{GF}$  collapses to a straight line although  $C_{GF} = 0$ , because  $\Delta g_m = 0$  by Eq. (58) or  $\Delta f_m = 0$  by Eq. (59). Specifically, when  $r = 1$ ,  $\Sigma_{GF}$  is the straight line between  $(0, 1)$  and  $(0, -1)$  and  $\Gamma_{GF}$  is the straight line between  $(0, 1)$  and  $(0, 0)$ , whereas when  $r = d$ ,  $\Sigma_{GF}$  is the straight line between  $(1, 0)$  and  $(-1, 0)$  and  $\Gamma_{GF}$  is the straight line between  $(1, 0)$  and  $(0, 0)$ .

Similarly, the normalized changes of the  $G(m)$  versus  $R(m)$  information–disturbance pair are derived from Eqs. (80) and (77) respectively as

$$\Delta r_m = \frac{\Delta R(m)}{\|\vec{\epsilon}_m\| \left\| \vec{\nabla} R(m) \right\|} = \frac{\vec{\epsilon}_m}{\|\vec{\epsilon}_m\|} \cdot \vec{r}_m. \quad (95)$$

The correlations between  $\Delta g_m$  and  $\Delta r_m$  are plotted in Fig. 5. The points were generated from 250 random modifications of six measurements in  $d = 4$  satisfying the conditions of Eqs. (21)–(23) with  $\|\vec{\epsilon}_m\| = 0.01$ . The ellipse  $\Sigma_{GR}$

$$\Sigma_{GR} : \quad \vec{\epsilon}_m = \epsilon \vec{g}_m \cos \phi + \epsilon \vec{r}_m \sin \phi \quad (96)$$

with  $0 \leq \phi < 2\pi$ , described by

$$(\Delta g_m)^2 + (\Delta r_m)^2 - 2C_{GR}\Delta g_m\Delta r_m = 1 - (C_{GR})^2, \quad (97)$$

has a tilt angle of  $-45^\circ$ . The shape of  $\Sigma_{GR}$  is characterized by  $C_{GR}$ , even though  $C_{GR}$  cannot be  $-1$  (unlike  $C_{GF}$ ). The points  $G^\pm$  and  $R^\pm$  correspond to  $\vec{\epsilon}_m = \epsilon \vec{g}_m^{(\pm)}$  and  $\vec{\epsilon}_m = \epsilon \vec{r}_m^{(\pm)}$ , respectively. Their coordinates are given by

$$\begin{aligned} G^+ : & \quad \left( 1 - \delta_{n_0, (d-1)}, -C_{GR}^{(+-)} \right), \\ R^+ : & \quad \left( C_{GR}^{(++)}, \cos \theta_r \right), \\ G^- : & \quad \left( -\cos \theta_g, -C_{GR}^{(--)} \right), \\ R^- : & \quad \left( C_{GR}^{(+-)}, -\delta_{n_0, 0} \right), \end{aligned} \quad (98)$$

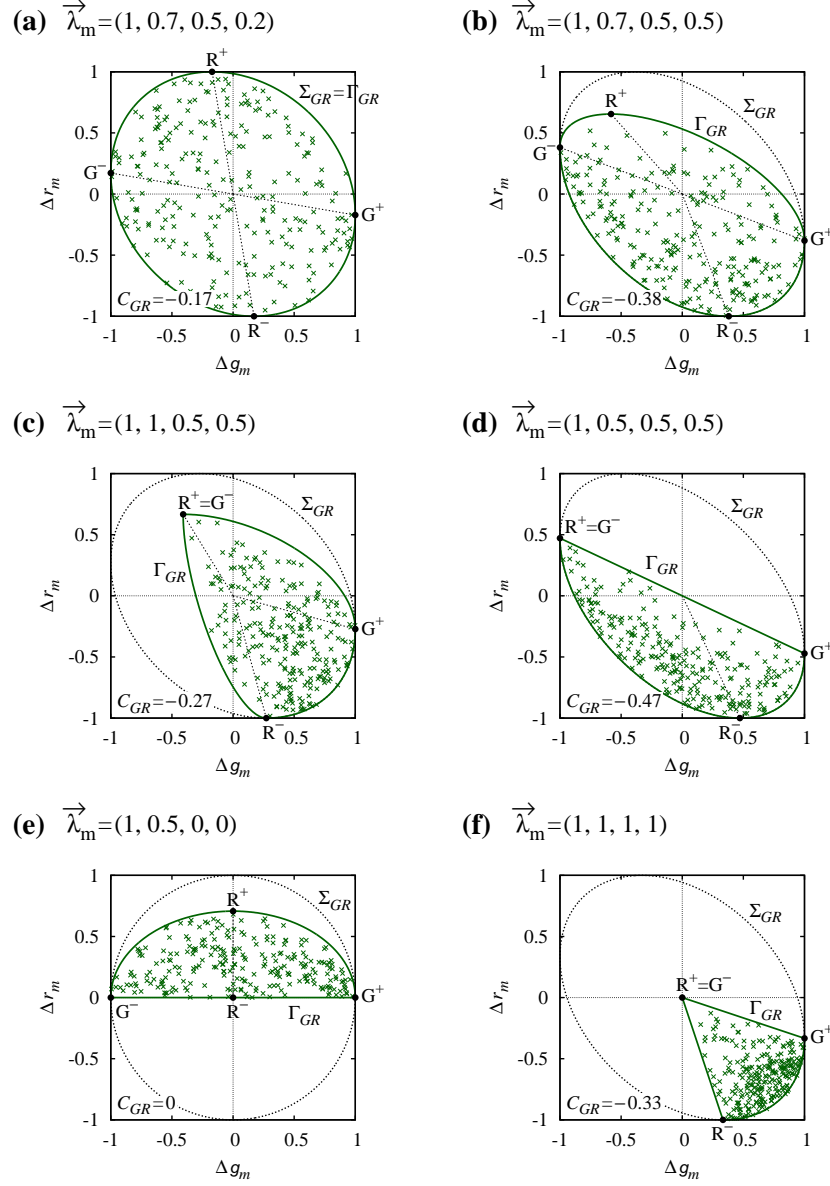


Figure 5: Correlations between  $\Delta g_m$  and  $\Delta r_m$  for six different measurements in  $d = 4$

where  $C_{GR}^{(+-)} = \vec{g}_m^{(+)} \cdot \vec{r}_m^{(-)}$  and  $C_{GR}^{(--)} = \vec{g}_m^{(-)} \cdot \vec{r}_m^{(-)}$  are respectively given by

$$C_{GR}^{(+-)} = -C_{GR} \geq 0, \quad (99)$$

$$C_{GR}^{(--)} = -\frac{\sqrt{n_1} \lambda_{m1} \lambda_{md} (1 - \delta_{n_1, d})}{\sqrt{(\sigma_m^2 - n_1 \lambda_{m1}^2) (\sigma_m^2 - \lambda_{md}^2)}} \leq 0. \quad (100)$$

If  $n_1 = n_d = 1$  and  $n_0 = 0$ , the plotted points are distributed throughout the whole region inside  $\Sigma_{GR}$  and the four points  $G^\pm$  and  $R^\pm$  are on  $\Sigma_{GR}$ . This situation is described in Fig. 5(a) for  $\vec{\lambda}_m = (1, 0.7, 0.5, 0.2)$ . Otherwise, under the conditions of Eqs. (21)–(23), the plotted points distribute only in a subregion of the region enclosed by  $\Sigma_{GR}$ . This scenario is illustrated in Fig. 5(b) for  $\vec{\lambda}_m = (1, 0.7, 0.5, 0.5)$  with  $n_d = 2$ , and in Fig. 5(c) for  $\vec{\lambda}_m = (1, 1, 0.5, 0.5)$  with  $n_1 = n_d = 2$ . Although  $G^+$  is always on  $\Sigma_{GR}$ ,  $R^+$  is not on  $\Sigma_{GR}$  if  $n_d > 1$ ,  $G^-$  is not on  $\Sigma_{GR}$  if  $n_1 > 1$ , and  $R^-$  is not on  $\Sigma_{GR}$  if  $n_0 > 0$ . The boundary  $\Gamma_{GR}$  of the subregion consists of four curves connecting the four points  $G^+$ ,  $R^+$ ,  $G^-$ , and  $R^-$ . These curves are generated by a similar equation to Eq. (89), but using  $\vec{r}_m^{(\pm)}$  instead of  $\vec{f}_m^{(\pm)}$ .

The shape of  $\Gamma_{GR}$  is characterized by four angles between the steepest directions:  $C_{GR}^{(++)}$ ,  $C_{GR}^{(--)}$ ,  $C_{GR}^{(+-)}$ , and  $C_{GR}^{(-+)} = \vec{g}_m^{(-)} \cdot \vec{r}_m^{(+)}$ . The latter is given by

$$C_{GR}^{(-+)} = \frac{\sqrt{n_1 n_d} \lambda_{m1} \lambda_{md} (1 - \delta_{n_d, d})}{\sqrt{(\sigma_m^2 - n_1 \lambda_{m1}^2) (\sigma_m^2 - n_d \lambda_{md}^2)}} \geq 0. \quad (101)$$

These terms are related as follows:

$$\begin{aligned} C_{GR}^{(++)} \cos \theta_r &= -C_{GR}^{(-+)} \cos \theta_g \cos \theta_r \\ &= C_{GR}^{(--)} \cos \theta_g = -C_{GR}^{(+-)} = C_{GR} \end{aligned} \quad (102)$$

if  $\vec{\lambda}_m \neq \vec{p}_d^{(d)}$ , and if  $\vec{\lambda}_m = \vec{p}_d^{(d)}$ ,  $C_{GR}^{(++)} = C_{GR}^{(-+)} = C_{GR}^{(--)} = 0$  and  $C_{GR} = -C_{GR}^{(+-)} = -1/(d-1)$ . Between  $G^+$  and  $R^+$ , the boundary  $\Gamma_{GR}$  is an arc of the ellipse described by

$$(\Delta g_m)^2 + (\Delta r'_m)^2 - 2C_{GR}^{(++)} \Delta g_m \Delta r'_m = 1 - [C_{GR}^{(++)}]^2, \quad (103)$$

where  $\Delta r'_m = \Delta r_m / \cos \theta_r$  and by Eq. (102) if  $\vec{\lambda}_m \neq \vec{p}_d^{(d)}$ . This ellipse is obtained by vertically compressing the ellipse  $\Sigma_{GR}$  in Eq. (97) by a factor of  $1/\cos \theta_r$  and replacing  $C_{GR}$  with  $C_{GR}^{(++)} = C_{GR} / \cos \theta_r$ . When  $C_{GR}^{(++)} = 0$ , this ellipse is untilted with axes 1 and  $\cos \theta_r$ , and when  $C_{GR}^{(++)} = -1$ , it collapses

to a straight line with slope  $-\cos\theta_r$ . Similarly,  $\Gamma_{GR}$  is an arc of the ellipse described by

$$(\Delta g'_m)^2 + (\Delta r'_m)^2 + 2C_{GR}^{(-+)}\Delta g'_m\Delta r'_m = 1 - \left[C_{GR}^{(-+)}\right]^2 \quad (104)$$

between  $R^+$  and  $G^-$ , an arc of the ellipse described by

$$(\Delta g'_m)^2 + (\Delta r_m)^2 - 2C_{GR}^{(--)}\Delta g'_m\Delta r_m = 1 - \left[C_{GR}^{(--)}\right]^2 \quad (105)$$

between  $G^-$  and  $R^-$  if  $\vec{\lambda}_m \neq \vec{p}_d^{(d)}$  and  $\lambda_{md} \neq 0$ , and an arc of  $\Sigma_{GR}$  with  $C_{GR} = -C_{GR}^{(+-)}$  between  $R^-$  and  $G^+$  if  $\lambda_{md} \neq 0$ . The cases of  $\vec{\lambda}_m = \vec{p}_d^{(d)}$  and  $\lambda_{md} = 0$  are anomalous, as discussed later.

Therefore, we can naturally represent the correlation between  $\Delta g_m$  and  $\Delta r_m$  by the four coefficients  $C_{GR}^{(++)}$ ,  $-C_{GR}^{(-+)}$ ,  $C_{GR}^{(--)}$ , and  $-C_{GR}^{(+-)}$ . For example, in Fig. 5(b),  $C_{GR}^{(++)} = -C_{GR}^{(-+)} = -0.58$  and  $C_{GR}^{(--)} = -C_{GR}^{(+-)} = -0.38$ , denoting that  $\Gamma_{GR}$  is flatter in the upper region of the straight line between  $G^+$  and  $G^-$  than in the lower region. In Fig. 5(c),  $R^+$  coincides with  $G^-$  because  $C_{GR}^{(-+)} = 1$ . For the optimal measurement  $\vec{\lambda}_m = (1, 0.5, 0.5, 0.5)$ ,  $\Gamma_{GR}$  is linear between  $G^+$  and  $R^+$  because  $C_{GR}^{(++)} = -1$  (see Fig. 5(d)). If  $n_1 = n_d = 1$  and  $n_0 = 0$ , the four coefficients are equal as shown in Fig. 5(a).

The cases of  $C_{GR} = 0$  and  $C_{GR}^{(++)} = 0$  are anomalous. The case of  $C_{GR} = 0$  occurs when  $\lambda_{md} = 0$ , for which  $C_{GR}^{(\pm\pm)} = 0$  with  $n_0 > 0$ . If  $\lambda_{md} = 0$  but  $\vec{\lambda}_m \neq \vec{p}_1^{(d)}$ ,  $\Sigma_{GR}$  is a circle but  $\Gamma_{GR}$  consists of two untilted elliptical arcs connecting  $(1, 0)$ ,  $(0, 1/\sqrt{n_d})$ , and  $(-\cos\theta_g, 0)$  with a straight line extending from  $(-\cos\theta_g, 0)$  to  $(1, 0)$  (see Fig. 5(e) for  $\vec{\lambda}_m = (1, 0.5, 0, 0)$ ) although  $C_{GR}^{(--)} = C_{GR}^{(-+)} = 0$ , because  $\vec{r}_m^{(-)} = \vec{0}$  by Eq. (53). If  $\vec{\lambda}_m = \vec{p}_1^{(d)}$ ,  $\Sigma_{GR}$  is a vertical straight line by Eq. (58) although  $C_{GR} = 0$  (as similarly observed in the  $G(m)$  versus  $F(m)$  correlations). Of course, when  $\lambda_{md} = 0$ ,  $\Delta R(m) = 0$  to first-order in  $\vec{\epsilon}_m$  even when  $\Delta r_m \neq 0$ , because

$$\left\| \vec{\nabla} R(m) \right\| = 0 \quad (106)$$

by Eq. (31). In contrast, the case of  $C_{GR}^{(++)} = 0$  occurs when not only  $\lambda_{md} = 0$  but also  $\vec{\lambda}_m = \vec{p}_d^{(d)}$ . If  $\vec{\lambda}_m = \vec{p}_d^{(d)}$ ,  $\Gamma_{GR}$  is the sector of the tilted ellipse  $\Sigma_{GR}$  with  $C_{GR} = -1/(d-1)$  (see Fig. 5(f)) although  $C_{GR}^{(++)} = C_{GR}^{(-+)} = C_{GR}^{(--)} = 0$ , because  $\cos\theta_r = \cos\theta_g = 0$  by Eqs. (59) and (60).

Figures 4 and 5 are consistent with the allowed regions of information versus disturbance in Ref. [19], and with the slopes of their boundaries in Ref. [20]. Figure 4(f) reproduces the neighborhood of point  $P_2$  in the single-outcome region of Fig. 1(a) in Ref. [19], and Fig. 4(b) reproduces the upper boundary (1, 3) around  $G(m) = 0.31$  without its lower neighborhood derived from the higher-order terms in  $\vec{\epsilon}_m$ . Meanwhile, Fig. 4(e) reproduces the lower boundary (2, 1) around  $G(m) = 0.29$ . The slopes  $\Delta f_m/\Delta g_m = -1$  in Fig. 4(b) and  $\Delta f_m/\Delta g_m = -\cos\theta_f/\cos\theta_g$  in Fig. 4(e) accord with the boundary slope  $dF(m)/dG(m)$  in Ref. [20] via Eqs. (29) and (30). Similarly, panels (d), (e), and (f) of Fig. 5 reproduce the upper boundary (1, 3) around  $G(m) = 0.31$ , the lower boundary  $R(m) = 0$  around  $G(m) = 0.36$ , and the neighborhood of point  $P_4$ , respectively, of Fig. 1(b) in Ref. [19]. The slope  $\Delta r_m/\Delta g_m = -\cos\theta_r$  in Fig. 5(d) accords with the boundary slope  $dR(m)/dG(m)$  in Ref. [20] via Eqs. (29) and (31).

## 6 Improvement

Finally, we attempt to increase the information extraction of a measurement while diminishing the disturbance. Although modifying a measurement to increase the information normally increases the disturbance, the information can plausibly be increased while decreasing the disturbance. Herein, we discuss a general improvement scheme in which the improvability is determined by the angle between the steepest directions of the information and disturbance.

We first improve a measurement  $\vec{\lambda}_m$  in terms of the  $G(m)$  versus  $F(m)$  information–disturbance pair. The modification  $\vec{\epsilon}_m$  should ensure positive values of  $\Delta G(m)$  in Eq. (64) and  $\Delta F(m)$  in Eq. (65). A best choice of  $\vec{\epsilon}_m$  is

$$\vec{\epsilon}_m = \epsilon \left( \vec{g}_m^{(+)} + \vec{f}_m^{(+)} \right), \quad (107)$$

which increases both  $G(m)$  and  $F(m)$  at the same ratio to Eqs. (67) and (69), respectively:

$$\Delta G(m) = \left( 1 + C_{GF}^{(++)} \right) [\Delta G(m)]_{\max} \geq 0, \quad (108)$$

$$\Delta F(m) = \left( 1 + C_{GF}^{(++)} \right) [\Delta F(m)]_{\max} \geq 0. \quad (109)$$

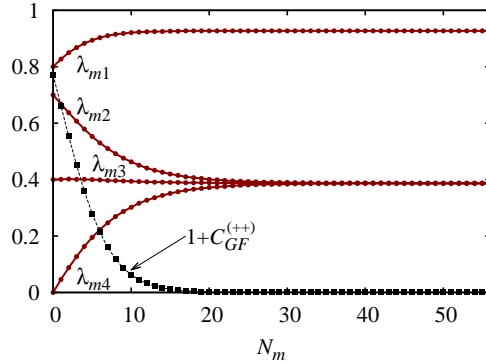


Figure 6: Transitions of  $\{\lambda_{mi}\}$  and  $1 + C_{GF}^{(++)}$  as functions of  $N_m$  in  $d = 4$

Thus, we can naturally define the improvability of a measurement as  $1 + C_{GF}^{(++)}$ . Clearly, the optimal measurements  $\vec{\lambda}_m = \vec{m}_{1,d-1}^{(d)}(\lambda)$  are not improvable because  $C_{GF}^{(++)} = -1$ . In fact, when  $C_{GF}^{(++)} = -1$ , no modification  $\vec{\epsilon}_m$  obtains  $\Delta G(m) > 0$  and  $\Delta F(m) > 0$ , because these modifications depart from the perfect negative correlation between  $\Delta g_m$  and  $\Delta f_m$  (see Fig. 4(b)). Unfortunately, being singular points of  $C_{GF}^{(++)}$ , the projective measurement  $\vec{\lambda}_m = \vec{p}_1^{(d)}$  and the identity operation  $\vec{\lambda}_m = \vec{p}_d^{(d)}$  are exceptions to this rule. These singular points cannot be improved even when  $C_{GF}^{(++)} = 0$ , because they have already reached the maximum  $G(m)$  or  $F(m)$ .

The modified measurement is also improvable if  $\vec{\lambda}'_m = \vec{\lambda}_m + \vec{\epsilon}_m$  yields  $C_{GF}^{(++)} \neq -1$ . The modification can be repeated until the measurement is optimized as  $C_{GF}^{(++)} = -1$ . For example, consider modifying a measurement  $\vec{\lambda}_m = (0.8, 0.7, 0.4, 0)$  by iterating Eq. (107) with  $\epsilon = 0.05$  in  $d = 4$ . Figure 6 shows the transitions of  $\{\lambda_{mi}\}$  and  $1 + C_{GF}^{(++)}$  as functions of  $N_m$ , where  $N_m$  is the number of modifications. As  $N_m$  increases,  $C_{GF}^{(++)}$  monotonously decreases to  $-1$  and exhibits no further change thereafter. At the resultant optimal measurement  $\vec{\lambda}_m = (0.93, 0.39, 0.39, 0.39)$ ,  $G(m)$  and  $F(m)$  increase from 0.30 and 0.76 respectively in the original measurement state to 0.33 and 0.87, respectively.

In general, an improved measurement has less improvability than the original measurement. For a general  $\vec{\epsilon}_m$ , the change in  $C_{GF}^{(++)}$  is related to

$\Delta G(m)$  and  $\Delta F(m)$  as

$$\Delta C_{GF}^{(++)} = \frac{(d+1)\sigma_m^4}{2(\tau_m\lambda_{m1} - \sigma_m^2)} \left[ \frac{\tau_m - \lambda_{m1}}{\lambda_{m1}(\sigma_m^2 - \lambda_{m1}^2)} \Delta G(m) + \frac{d\lambda_{m1} - \tau_m}{\tau_m(d\sigma_m^2 - \tau_m^2)} \Delta F(m) \right] C_{GF}^{(++)}. \quad (110)$$

Note that in this expression,  $\Delta C_{GF}^{(++)} < 0$  if  $\Delta G(m) > 0$  and  $\Delta F(m) > 0$ . Equation (110) can be proven by expanding  $\Delta G(m)$ ,  $\Delta F(m)$ , and  $\Delta C_{GF}^{(++)}$  in terms of  $\Delta\lambda_{m1}$ ,  $\Delta\tau_m$ , and  $\Delta\sigma_m^2$ :

$$\Delta G(m) = \frac{2}{d+1} \left[ \frac{\lambda_{m1}}{\sigma_m^2} \left( \Delta\lambda_{m1} - \frac{\lambda_{m1}}{2\sigma_m^2} \Delta\sigma_m^2 \right) \right], \quad (111)$$

$$\Delta F(m) = \frac{2}{d+1} \left[ \frac{\tau_m}{\sigma_m^2} \left( \Delta\tau_m - \frac{\tau_m}{2\sigma_m^2} \Delta\sigma_m^2 \right) \right], \quad (112)$$

and the term  $\Delta C_{GF}^{(++)}$  can be expanded similarly.

We now consider the  $G(m)$  versus  $R(m)$  information–disturbance pair. A best choice of  $\vec{\epsilon}_m$  is

$$\vec{\epsilon}_m = \epsilon \left( \vec{g}_m^{(+)} + \vec{r}_m^{(+)} \right), \quad (113)$$

which increases both  $G(m)$  and  $R(m)$  at the same ratio to Eqs. (67) and (79), respectively:

$$\Delta G(m) = \left( 1 + C_{GR}^{(++)} \right) [\Delta G(m)]_{\max} \geq 0, \quad (114)$$

$$\Delta R(m) = \left( 1 + C_{GR}^{(++)} \right) [\Delta R(m)]_{\max} \geq 0. \quad (115)$$

As in the  $G(m)$  versus  $F(m)$  correlation, we can naturally define the improvability of a measurement by  $1 + C_{GR}^{(++)}$ . The optimal measurements  $\vec{\lambda}_m = \vec{m}_{1,d-1}^{(d)}(\lambda)$  are not improvable because  $C_{GR}^{(++)} = -1$ . In fact, when  $C_{GR}^{(++)} = -1$ , no modification  $\vec{\epsilon}_m$  obtains  $\Delta G(m) > 0$  and  $\Delta R(m) > 0$ , because these modifications depart from the linearity of  $\Gamma_{GR}$  between  $G^+$  and  $R^+$  (see Fig. 5(d)). Being singular points of  $C_{GR}^{(++)}$ , the projective measurement  $\vec{\lambda}_m = \vec{p}_1^{(d)}$  and the identity operation  $\vec{\lambda}_m = \vec{p}_d^{(d)}$  are exceptions to this rule. These singular points cannot be improved even when  $C_{GR}^{(++)} = 0$ , because they have already reached the maximum  $G(m)$  or  $R(m)$ .

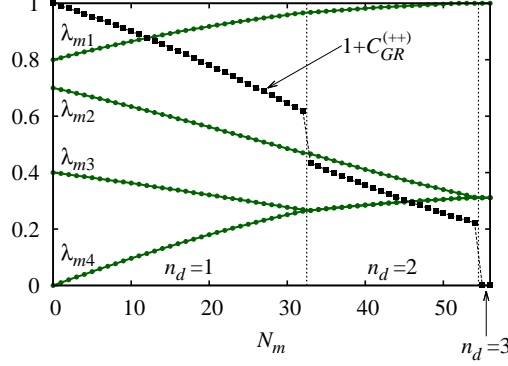


Figure 7: Transitions of  $\{\lambda_{mi}\}$  and  $1 + C_{GR}^{(++)}$  as functions of  $N_m$  in  $d = 4$

The modification can be repeated until the measurement is optimized as  $C_{GR}^{(++)} = -1$ . For example, consider modifying  $\vec{\lambda}_m = (0.8, 0.7, 0.4, 0)$  by iterating Eq. (113) with  $\epsilon = 0.01$  in  $d = 4$ . Figure 7 shows the transitions of  $\{\lambda_{mi}\}$  and  $1 + C_{GR}^{(++)}$  as functions of  $N_m$ . Although  $C_{GR}^{(++)}$  discontinuously jumps at each change in  $n_d$ , it monotonously decreases to  $-1$  with increasing  $N_m$  until  $n_d = d - 1$ . At this point,  $C_{GR}^{(++)}$  becomes  $-1$  and no further change occurs. If  $\lambda_{m1} > 1$  after a modification,  $\vec{\lambda}_m$  is renormalized to  $\lambda_{m1} = 1$  by the rescaling operation in Eq. (17). Moreover, if  $\lambda_{m(4-n_d)} < \lambda_{m4}$  after a modification and the descending order is broken, the modification is redone using a temporarily reduced  $\epsilon$  satisfying  $\lambda_{m(4-n_d)} = \lambda_{m4}$  to increase  $n_d$ . At the resultant optimal measurement  $\vec{\lambda}_m = (1, 0.31, 0.31, 0.31)$ ,  $G(m)$  and  $R(m)$  increase from 0.30 and 0 respectively in the original measurement state to 0.35 and 0.30, respectively.

As observed for the  $G(m)$  versus  $F(m)$  correlations, an improved measurement has less improvability than the original measurement. For a general  $\vec{\epsilon}_m$  that does not change  $n_d$ , the change in  $C_{GR}^{(++)}$  is related to  $\Delta G(m)$  and  $\Delta R(m)$  as

$$\Delta C_{GR}^{(++)} = \frac{\sigma_m^4}{2} \left[ \frac{d+1}{\lambda_{m1}^2 (\sigma_m^2 - \lambda_{m1}^2)} \Delta G(m) + \frac{1}{d\lambda_{md}^2 (\sigma_m^2 - n_d \lambda_{md}^2)} \Delta R(m) \right] C_{GR}^{(++)}. \quad (116)$$

Note that in this expression,  $\Delta C_{GR}^{(++)} < 0$  if  $\Delta G(m) > 0$  and  $\Delta R(m) > 0$ . Equation (116) can be proven by expanding  $\Delta G(m)$ ,  $\Delta R(m)$ , and  $\Delta C_{GR}^{(++)}$  in terms of  $\Delta\lambda_{m1}$ ,  $\Delta\lambda_{md}$ , and  $\Delta\sigma_m^2$ : Eq. (111),

$$\Delta R(m) = 2d \left[ \frac{\lambda_{md}}{\sigma_m^2} \left( \Delta\lambda_{md} - \frac{\lambda_{md}}{2\sigma_m^2} \Delta\sigma_m^2 \right) \right], \quad (117)$$

and similarly for  $\Delta C_{GR}^{(++)}$ .

Importantly, the modifications given by Eqs. (107) and (113) only slightly change the probability of the outcome  $m$  in Eq. (6). As a function of  $\vec{\lambda}_m$ , the probability is calculated as  $p(m) = \sigma_m^2/d$ . After a modification  $\vec{\epsilon}_m$ , this probability becomes  $\Delta p(m) = 2\vec{\epsilon}_m \cdot \vec{\lambda}_m/d$  (to first-order in  $\vec{\epsilon}_m$ ). By Eqs. (54)–(56), this probability equals 0 in Eqs. (107) and (113), although  $p(m)$  increases by the second-order term in  $\vec{\epsilon}_m$  and decreases when rescaled by Eq. (17) with  $\lambda_{m1} > 1$ . In practice,  $p(m)$  increases from 0.32 to 0.33 in the case of Fig. 6 and by less than 0.01 in the case of Fig. 7.

## 7 Summary

We discussed the local trade-off between information and disturbance in quantum measurements described by a measurement operator  $\hat{M}_m$ . As functions of the singular values  $\vec{\lambda}_m$  of  $\hat{M}_m$ , the information was quantified by the estimation fidelity  $G(m)$ , whereas the disturbance was quantified by the operation fidelity  $F(m)$  and by the physical reversibility  $R(m)$ . The steepest ascent and descent directions of the information and disturbance were derived from their unit gradient vectors. When a measurement is modified to enhance the information, increased disturbance in the system is the trade-off. The present study investigated the local trade-off between  $G(m)$  and  $F(m)$  and between  $G(m)$  and  $R(m)$  by plotting their normalized changes on a plane for various modifications of a measurement. Finally, the modifications were optimized to enhance the information gain while diminishing the disturbance.

The above results are entirely general and fundamental to the quantum theory of measurements. They are applicable to any single-outcome process of an arbitrary measurement, based neither on averaging over outcomes nor optimizing over measurements. Consequently, they can broaden our perspectives on quantum measurements, and are potentially useful tools for quantum information processing and communication.

## References

- [1] C. A. Fuchs and A. Peres, Phys. Rev. A **53**, 2038 (1996).
- [2] K. Banaszek, Phys. Rev. Lett. **86**, 1366 (2001).
- [3] C. A. Fuchs and K. Jacobs, Phys. Rev. A **63**, 062305 (2001).
- [4] K. Banaszek and I. Devetak, Phys. Rev. A **64**, 052307 (2001).
- [5] H. Barnum, arXiv:quant-ph/0205155.
- [6] G. M. D'Ariano, Fortschr. Phys. **51**, 318 (2003).
- [7] M. Ozawa, Ann. Phys. (NY) **311**, 350 (2004).
- [8] M. G. Genoni and M. G. A. Paris, Phys. Rev. A **71**, 052307 (2005).
- [9] L. Mišta, Jr., J. Fiurášek, and R. Filip, Phys. Rev. A **72**, 012311 (2005).
- [10] L. Maccone, Phys. Rev. A **73**, 042307 (2006).
- [11] M. F. Sacchi, Phys. Rev. Lett. **96**, 220502 (2006).
- [12] F. Buscemi and M. F. Sacchi, Phys. Rev. A **74**, 052320 (2006).
- [13] K. Banaszek, Open Syst. Inf. Dyn. **13**, 1 (2006).
- [14] F. Buscemi, M. Hayashi, and M. Horodecki, Phys. Rev. Lett. **100**, 210504 (2008).
- [15] Y. W. Cheong and S.-W. Lee, Phys. Rev. Lett. **109**, 150402 (2012).
- [16] X.-J. Ren and H. Fan, J. Phys. A: Math. Theor. **47**, 305302 (2014).
- [17] L. Fan, W. Ge, H. Nha, and M. S. Zubairy, Phys. Rev. A **92**, 022114 (2015).
- [18] T. Shitara, Y. Kuramochi, and M. Ueda, Phys. Rev. A **93**, 032134 (2016).
- [19] H. Terashima, Quantum Inf. Process. **16**, 250 (2017).
- [20] H. Terashima, Quantum Inf. Process. **18**, 63 (2019).

- [21] H. Terashima, Phys. Rev. A **93**, 022104 (2016).
- [22] M. A. Nielsen and I. L. Chuang, *Quantum Computation and Quantum Information* (Cambridge University Press, Cambridge, 2000).
- [23] M. A. Nielsen and C. M. Caves, Phys. Rev. A **55**, 2547 (1997).
- [24] M. Ueda, N. Imoto, and H. Nagaoka, Phys. Rev. A **53**, 3808 (1996).
- [25] M. Ueda, in *Frontiers in Quantum Physics: Proceedings of the International Conference on Frontiers in Quantum Physics, Kuala Lumpur, Malaysia, 1997*, edited by S. C. Lim, R. Abd-Shukor, and K. H. Kwek (Springer, Singapore, 1998), pp. 136–144.
- [26] M. Koashi and M. Ueda, Phys. Rev. Lett. **82**, 2598 (1999).